The Structures of $M_2X_9^{3-}$ (M=Bi ; X=Cl, Br) Ions Determined by Rietveld Analysis of X-Ray Powder Diffraction Data

Hideta ISHIHARA,* Koji YAMADA,† Tsutomu OKUDA,† and Alarich WEISS††
Department of Chemistry, Faculty of Education, Saga University, Honjo-machi 1, Saga 840
† Department of Chemistry, Faculty of Science, Hiroshima University, Kagamiyama, Higasihiroshima, Hiroshima 724
†† Institüt für Physikalische Chemie, Physikalische Chemie III, Technische Hochschule Darmstadt, D-6100 Darmstadt, Germany

(Received August 18, 1992)

The results of the Rietveld analysis of X-ray powder diffraction data for title compounds show that the space group for $(CH_3NH_3)_3Bi_2Cl_9$ is *Pnma* with $Z=4$ and its lattice constants are $a=2040.6$, $b=770.0$, $c=1324.6$ pm. It consists of one-dimensional double chains of $Bi_2Cl_9^{3-}$ polyanions. The space group for $[N(CH_3)_4]_3Bi_2X_9$ (X=Cl, Br) is $P6_3/mmc$ with $Z=2$ and its lattice constants are $a=926.2$, $c=2192.2$ pm for X=Cl and $a=951.8$, $c=2245.9$ pm for X=Br. It contains ioslated $Bi_2X_9^{3-}$ anions with a triple bridged bioctahedral structure.

At present four types of structures of $M_2X_9^{3-}$ (M = Sb, Bi; X = Cl, Br) ions are known: (1) one-dimensional double chains of polyanions like in $(CH_3NH_3)_3Sb_2Cl_9$,[1] (2) two-dimensional layers of polyanions as in $Cs_3Bi_2Br_9$[2] and $(CH_3NH_3)_3M_2Br_9$ (M = Sb, Bi),[3] (3) isolated confacial bioctahedral $M_2X_9^{3-}$ anions as found in $[N(CH_3)_4]_3Sb_2X_9$ (X = Cl, Br),[3,4] and (4) two-dimensional layers consist of $SbCl_3$ units connected by Cl^- anions like in $[NH(CH_3)_3]_3Sb_2Cl_9$ and $[NH_2(CH_3)_2]_3Sb_2Cl_9$.[5,6] In this study, we tried to investigate the structures of $A_3Bi_2X_9$ (A=alkylammonium cations) in more detail.

Experimental

The preparation of $(CH_3NH_3)_3Bi_2Cl_9$, $[N(CH_3)_4]_3Bi_2Cl_9$, and $[N(CH_3)_4]_3Bi_2Br_9$ and their identification were described elsewhere.[3] Their X-ray powder diffraction patterns were obtained by using a Rigaku Rad-B system. The measurements were carried out at about 295 K with a step-scan interval of 0.02° at the scanning speed of 0.4° min^{-1} using Cu K_α radiation. The data were collected using 0.5° divergence- and receiving-slit aperture. The computer program used for Rietveld analysis was developed by Izumi.[7] Rietveld refinements were done using dummy atoms instead of alkylammonium cations, because thermal rotational motion of the cations takes place at room temperature,[1,3] which leads to allocation of atoms contained in the cations at the disordered positions. Although a procedure using cellulosic adhesive-acetone resin was adopted to get random orientation of crystallite,[7] in the case of $[N(CH_3)_4]_3Bi_2X_9$ (X=Cl and Br) and $(CH_3NH_3)_3Bi_2Cl_9$, preferred orientation had to be corrected according to the platy and needle-like crystal habit, respectively. Figure 1 shows the final best-fit profiles together with the raw data. The crystallographic parameters and experimental details are listed in Table 1, the positional and thermal parameters in Table 2, and the structural parameters (some bond distances and angles) in Table 3.

Results and Discussion

Tris(monomethylammonium) Enneachlorodibismuthate(III), $(CH_3NH_3)_3Bi_2Cl_9$. $(CH_3NH_3)_3Bi_2Cl_9$ is isomorphous with its Sb analogue[1] at room temperature as reported by Jakubas et al.[8] and also

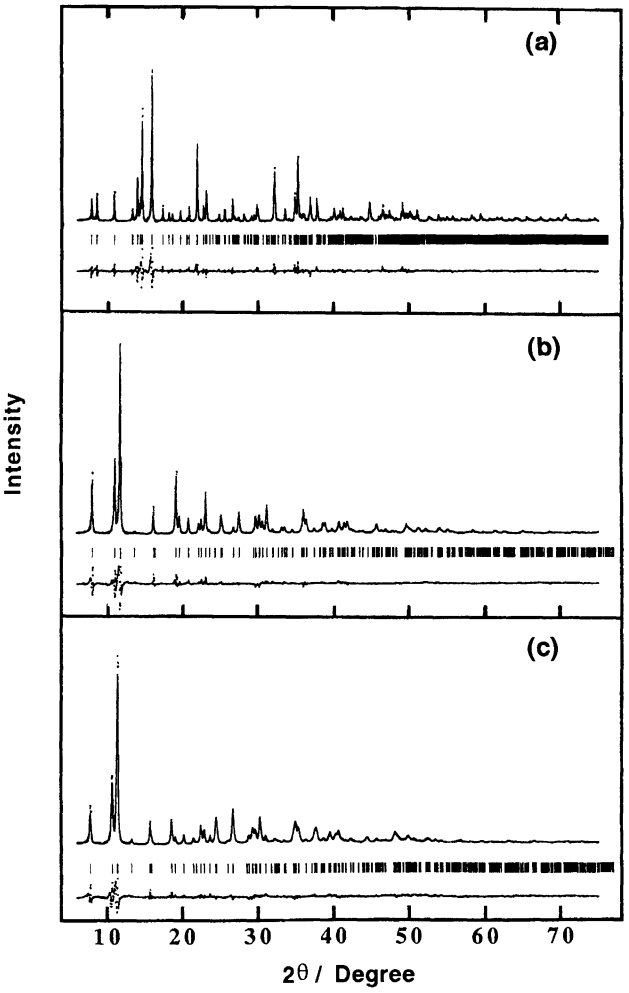

Fig. 1. Final difference plots of the Rietveld analysis of (a) : $(CH_3NH_3)_3Bi_2Cl_9$, (b) : $[N(CH_3)_4]_3Bi_2Cl_9$, (c) : $[N(CH_3)_4]_3Bi_2Br_9$. In the upper portion the observed data are shown by dots; the calculated patterns are given by the solid line. The lower parts are plots of the difference. The intensity are given in arbitrary unit.

Table 1. Experimental Conditions and Some Crystallographic Data of $(CH_3NH_3)_3Bi_2Cl_9$, $[N(CH_3)_4]_3Bi_2Cl_9$, and $[N(CH_3)_4]_3Bi_2Br_9$. Diffractometer: Rigaku Rad-B: Radiation: Cu K_α. The Rietveld refinements were carried out using a dummy atom in place of the alkylammonium cations.

Formula	$C_3H_{18}Bi_2Cl_9N_3$	$C_{12}H_{36}Bi_2Cl_9N_3$	$C_{12}H_{36}Bi_2Br_9N_3$
F. W.	833.22	959.47	1359.53
Range 2θ/°	6—75	6—75	6—75
Step width/°	0.02	0.02	0.02
R_F/%[a]	3.39	4.35	3.55
R_p/%[b]	9.66	8.47	6.37
R_{wp}/%[c]	13.20	11.73	8.73
R_e/%[d]	6.85	6.57	5.50
Number of structural parameters	35	12	12
Number of atoms	11	5	5
Lattice constants a/pm	2040.6(1)	926.2(0)	951.8(1)
b/pm	770.0(0)		
c/pm	1324.6(0)	2192.2(1)	2245.9(2)
Space group	D_{2h}^{16}-$Pnma$	D_{6h}^{4}-$P6_3/mmc$	D_{6h}^{4}-$P6_3/mmc$
Z	4	2	2
$\rho_{calcd}/(Mg\,m^{-3})$	2.659(1)	1.957(1)	2.563(1)
$\rho_{obsd}/(Mg\,m^{-3})$	2.40	1.87	2.43
$V/(10^6 pm^3)$	2081.4(1)	1628.6(1)	1762.1(5)

a) $R_F=\Sigma_k|[I_k(obsd)]^{1/2}-[I_k(calcd)]^{1/2}|/\Sigma_k[I_k(obsd)]^{1/2}$, where $I_k(obsd)$ and $I_k(calcd)$ are the integrated observed and calculated intensites, respectively. b) $R_p=\Sigma_i|y_i(obsd)-y_i(calcd)|/\Sigma_i y_i(obsd)$ where $y_i(obsd)$ are observed intensities and $y_i(calcd)$ calculated intensities. c) $R_{wp}=\{\Sigma_i w_i[y_i(obsd)-y_i(calcd)]^2/\Sigma_i w_i y_i^2]\}^{1/2}$. d) R_e is the expected R_{wp}.

Table 2. Positional and Isotropic Thermal Partmeter

2a) Positional and isotropic thermal parameters, U, with standard deviation in $(CH_3NH_3)_3Bi_2Cl_9$.

Atom	Position[a]	x	y	z	U/pm^2
Bi(1)	4c	0.0045(3)	0.2500	0.7601(5)	196(30)
Bi(2)	4c	−0.1711(3)	0.2500	0.4275(6)	149(29)
Cl(1)	4c	−0.0709(21)	0.2500	0.5898(32)	168(111)[b]
Cl(2)	4c	−0.2503(21)	0.2500	0.2830(28)	279(73)[b]
Cl(3)	4c	0.0743(22)	0.2500	0.9234(31)	279[b]
Cl(4)	8d	−0.0664(13)	0.4847(61)	0.8428(17)	279[b]
Cl(5)	8d	−0.2359(12)	0.0103(51)	0.5341(18)	279[b]
Cl(6)	8d	0.0938(13)	−0.0118(52)	0.6845(18)	168[b]
K(1)[c]	4c	0.0980(40)	0.2500	0.3962(92)	7976(1028)
K(2)[c]	4c	0.2596(36)	0.2500	0.7777(74)	4474(529)
K(3)[c]	4c	0.4061(29)	0.2500	0.4483(56)	3273(437)

a) Multiplicity and Wyckoff notation. b) Thermal parameters were constrained as follows; $U(Cl(1))=U(Cl(6))$, $U(Cl(2))=U(Cl(3))=U(Cl(4))=U(Cl(5))$. c) K atoms used as dummy atoms for the refinement.

2b) Positional and isotropic thermal parameters, U, with standard deviation in $[N(CH_3)_4]_3Bi_2Cl_9$.

Atom	Position[a]	x	y	z	U/pm^2
Bi	4f	0.3333	0.6667	0.1617(4)	540(41)
Cl(1)	6h	0.4683(23)	0.9367	0.2500	819(181)
Cl(2)	12k	0.1966(20)	0.3932	0.0994(11)	1120(161)
Cs(1)[b]	2b	0.0000	0.0000	0.2500	12235(637)
Cs(2)[b]	4f	0.6667	0.3333	0.0886(16)	11866(586)

a) Multiplicity and Wyckoff notation. b) Cs atoms used as dummy atoms for the refinement.

2c) Positional and isotropic thermal parameters, U, with standard deviation in $[N(CH_3)_4]_3Bi_2Br_9$.

Atom	Position[a]	x	y	z	U/pm^2
Bi	4f	0.3333	0.6667	0.1602(4)	409(49)
Br(1)	6h	0.4713(9)	0.9426	0.2500	577(90)
Br(2)	12k	0.1945(9)	0.3891	0.0956(5)	966(85)
Cs(1)[b]	2b	0.0000	0.0000	0.2500	15312(800)
Cs(2)[b]	4f	0.6667	0.3333	0.0917(16)	12841(518)

a) Multiplicity and Wyckoff notation. b) Cs atoms used as dummy atoms for the refinement.

Table 3. Bond Distances and Angels

3a) Bond distances (pm) and angles (°) with standard deviations in parentheses for $(CH_3NH_3)_3Bi_2Cl_9$.

Bi(1)–Cl(1)	273.0(43)	Bi(2)–Cl(1)	296.6(43)
Bi(1)–Cl(3)	259.0(45)	Bi(2)–Cl(2)	250.6(38)
Bi(1)–Cl(4)	256.2(39)	Bi(2)–Cl(5)	267.5(32)
Bi(1)–Cl(6)	289.6(32)	Bi(2)–Cl(6^{ii})	283.8(30)
Cl(1)–Bi(1)–Cl(4)	92.0(8)	Cl(1)–Bi(2)–Cl(5)	87.6(8)
Cl(1)–Bi(1)–Cl(6)	93.9(8)	Cl(1)–Bi(2)–Cl(6^{ii})	89.8(8)
Cl(3)–Bi(1)–Cl(4)	87.3(8)	Cl(2)–Bi(2)–Cl(5)	94.8(9)
Cl(3)–Bi(1)–Cl(6)	86.7(9)	Cl(2)–Bi(2)–Cl(6^{ii})	87.7(9)
Cl(4)–Bi(1)–Cl(4^{i})	89.7(17)	Cl(6^{ii})–Bi(2)–Cl(6^{iii})	80.5(15)
Cl(6)–Bi(1)–Cl(6^{i})	88.2(14)	Cl(5)–Bi(2)–Cl(5^{i})	87.3(14)
Cl(4)–Bi(1)–Cl(6)	90.7(12)	Cl(5)–Bi(2)–Cl(6^{ii})	96.0(10)

Symmetry codes: i) $x,1/2-y,z$; ii) $-x,-y,1-z$; iii) $-x,1/2+y,1-z$.

3b) Bond distances (pm) and angles (°) with standard deviations in parentheses for $[N(CH_3)_4]_3Bi_2X_9$ (X=Cl and Br).

Bi–Cl(1)[a]	290.6(28)	Bi–Br(1)[a]	304.0(12)
Bi–Cl(2)[b]	258.4(30)	Bi–Br(2)[b]	270.9(13)
Bi···Bi(^{i})	387.3(19)	Bi···Bi(^{i})	403.5(18)
Bi–Cl(1)–Bi(^{i})	83.6(10)	Bi–Br(1)–Bi(^{i})	83.2(5)
Cl(2)–Bi–Cl(2^{ii})	94.6(8)	Br(2)–Bi–Br(2^{ii})	94.0(5)
Cl(2)–Bi–Cl(1^{i})	92.1(5)	Br(2)–Bi–Br(1^{i})	92.3(2)
Cl(1)–Bi–Cl(1^{i})	80.4(8)	Br(1)–Bi–Br(1^{i})	80.8(4)
Cl(1)–Bi–Cl(2)	170.1(9)	Br(1)–Bi–Br(2)	170.8(5)

a) Bridging chlorine(bromine) atom.
b) Terminal chlorine(bromine) atom.
Symmetry codes: i) $1-y,1+x-y,1/2-z$; ii) $1-y,1+x-y,z$.

with the β-modification of $Cs_3Sb_2Cl_9$,[9] although the latter two structures are refined on the basis of the space group Pmcn. It consists of one-dimensional double chains of polyanions as shown in Fig. 2. Each Bi atom is surrounded by six Cl atoms. The Bi atoms linked by the bridging chlorine Cl(6) atoms form zigzag chains along the a-axis, and two parallel zigzag chains are linked via Cl(1) atoms, which leads to one-dimensional polymers. Between stacks with rectangular cross sections, there are three types of cation sites. The cations $CH_3NH_3^+$ show some rotational motions like in the Sb analogue.[1] Provided that the dummy atoms are located at the center of the mobile $CH_3NH_3^+$ cations, a closed-packed arrangement is formed by chlorine and the dummy atoms with the layer running in the bc plane, and Bi atoms occupy the octahedral holes of the chlorine sublattice as found in the β-modification of $Cs_3Bi_2Cl_9$.

Tris(tetramethylammonium) Enneachlorodibismuthate(III) and Tris(tetramethylammonium) Enneabromodibismuthate(III), $[N(CH_3)_4]_3Bi_2Cl_9$ and $[N(CH_3)_4]_3Bi_2Br_9$. $[N(CH_3)_4]_3Bi_2X_9$ (X = Cl and Br) are isomorphous with the Sb analogues.[3,4] They contain $Bi_2X_9^{3-}$ anions which have D_{3h} symmetry and a triple-bridged bioctahedral structure as shown in Fig. 3. The cations show isotropic rotation at room temperature like in the Sb analogues.[3]

There are apparent differences between the structures of $Bi_2X_9^{3-}$ and $Sb_2X_9^{3-}$ ions: Terminal Bi–X^t (X=Cl and Br) bonds are longer than Sb–X^t bonds, the bond angles of X^t–Bi–X^t (X^t=terminal halogen) and Bi–X^b–Bi (X^b=bridging halogen) are larger than corresponding angles in Sb analogues. On the other hand, the dif-

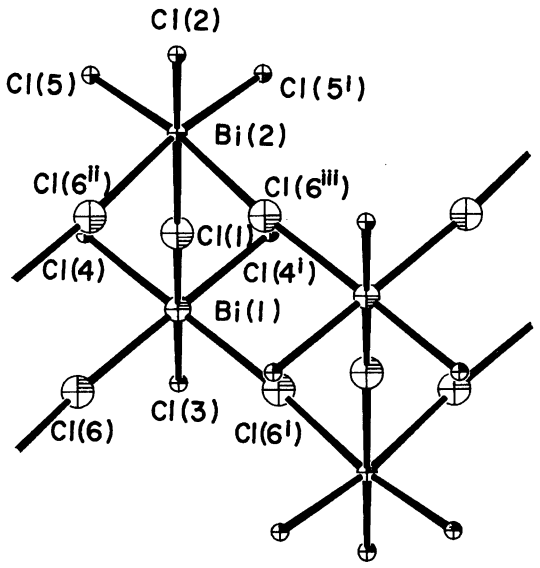

Fig. 2. Structure of the polyanion in $(CH_3NH_3)_3Bi_2Cl_9$.

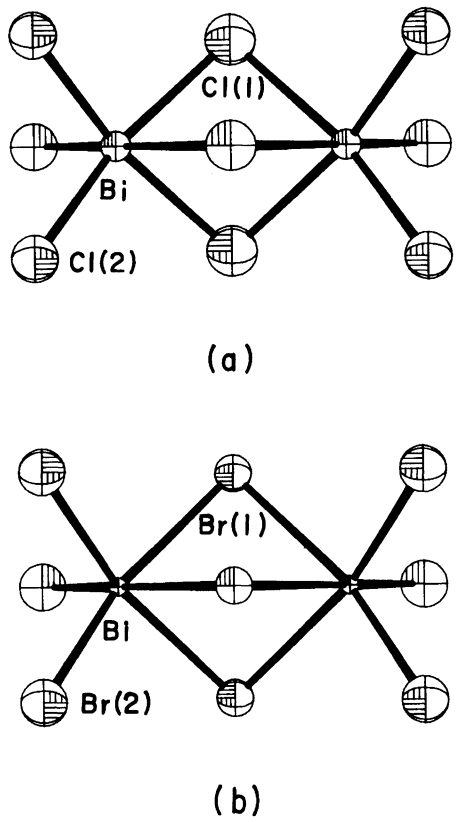

Fig. 3. Structures of the anions (a): $Bi_2Cl_9^{3-}$ in $[N(CH_3)_4]_3Bi_2Cl_9$, (b): $Bi_2Br_9^{3-}$ in $[N(CH_3)_4]_3Bi_2Br_9$.

ference between Bi–X^b bond lengths (290.5(28) pm for X=Cl and 304.0(12) pm for X=Br) and Sb–X^b bond lengths (293.4(9) pm for X=Cl and 305.1(4) pm for X=Br) is not significant if the estimated standard deviations are taken into consideration, although the Bi–X (X=Cl, Br, and I) bonds are usually longer than those in corresponding Sb compounds.[10] The results of the observation of nuclear quadrupole resonance (NQR) show that the electronic charge of the Br^b atom in $[N(CH_3)_4]_3Bi_2Br_9$ is smaller than that of the Br^b atom in the Sb analogue.[3] The imbalance of 4p-electrons of Br atoms, U_p for the bridging bromine atoms was calculated according to the following equation:

$$U_p = (e^2Qq_{obsd})/(e^2Qq_p) = 2 - N_z, \quad (1)$$

where e^2Qq_{obsd}/h and e^2Qq_p/h are the observed quadrupole coupling constant and the atomic quadrupole coupling constant of Br, respectively, and N_z is the occupation number of the 4p-orbital of the Br atom. The net charge is equal to $1-N_z$. In this case, $e^2Qq_{obsd}/h \approx 2\nu$ where ν is the observed NQR frequency, at 298 K $\nu(^{81}Br) = 41.37$ MHz for $[N(CH_3)_4]_3Bi_2Br_9$ and $\nu(^{81}Br) = 39.70$ MHz for $[N(CH_3)_4]_3Sb_2Br_9$. Therefore the repulsion between the bridging atoms in the Bi compound diminish and then the angle of Bi–Br^b–Bi, 83.2°, increases to a larger value than that of Sb–Br^b–Sb, 80.9°, and the decrease in the repulsion also increases the angle of Br^t–Bi–Br^t, 94.0°, to a higher value than that of Br^t–Sb–Br^t, 92.7°. This phenomenon is also significant for the chloride: 83.6° for Bi–Cl^b–Bi compared with 80.8° for Sb–Cl^b–Sb, and 94.6° for Cl^t–Bi–Cl^t compared with 91.4° for Cl^t–Sb–Cl^t. The size of a halogen atom has an influence on the structure of an $M_2X_9^{3-}$ ion. In the case of M=Sb, the Sb–Sb separations increases in the order F<Cl<Br<I,[4] and the angle Sb–Br^b–Sb also increases in this order. In the case of the transition metal $M_2X_9^{3-}$ species, an ideal situation where M–X^b and M–X^t distances are equal gives an angle M–X^b–M of 70.53°.[11] In the case of main group elements, the M–X^b–M angles are larger than 70.53° because of the absence of the metal-metal bond. The Sb–X^b–Sb angles and Sb–Sb distance increase with increasing X–X repulsion.

Hideta Ishihara expresses his thanks to the Alexander von Humboldt Stiftung for a research fellowship.

References

1) R. Jakubas, Z. Czapla, Z. Galewski, L. Sobczyk, O. J. Zogal, and T. Lis, *Phys. Status Solidi A*, **93**, 449(1986).
2) F. Lazarini, *Acta Crystallogr., Sect. B*, **33**, 2961 (1977).
3) H. Ishihara, K. Watanabe, A. Iwata, K. Yamada, Y. Kinoshita, T. Okuda, V. G. Krishnan, S. Dou, and Al. Weiss, *Z. Naturforsch., A*, **47a**, 65 (1992).
4) M. Hall, M. Nunn, M. J. Begley, and D. B. Sowerby, *J. Chem. Soc., Dalton Trans.*, **1986**, 1231.
5) A. Kallel and J. W. Bats, *Acta Crystallogr., Sect. C*, **41**, 1022 (1985).
6) M. Gdaniec, Z. Kosturkiewicz, R. Jakubas, and L. Sobczyk, *Ferroelectrics*, **77**, 31 (1988).
7) F. Izumi, M. Mitomo, and Y. Bando, *J. Mater. Sci.*, **19**, 3115 (1984)., The analysis was made using the "RIETAN" program, written by F. Izumi, The adopted precedure to get random orientation of crystallite is desribed in the manual of "RIETAN".
8) R. Jakubas, J. Zaleski, and L. Sobczyk, *Ferroelectrics*, **108**, 109 (1990).
9) K. Kihara and T. Sudo, *Acta Crystallogr., Sect. B*, **30**, 1088 (1974).
10) See Ref. 3. They compared the Bi–X bond lengths with the Sb–X bond lengths on the basis of the bond-order.
11) F. A. Cotton and D. A. Ucko, *Inorg. Chim. Acta*, **6**, 161 (1972).